



A thorny tale: The origin and diversification of *Cirsium* (Compositae)

Lucía D. Moreyra^{a,*}, Alfonso Susanna^a, Juan Antonio Calleja^b, Jennifer R. Ackerfield^c, Turan Arabacı^d, Carme Blanco-Gavaldà^e, Christian Brochmann^f, Tuncay Dirmenci^g, Kazumi Fujikawa^h, Mercè Galbany-Casals^e, Tiangang Gaoⁱ, Abel Gizaw^{f,j}, Iraj Mehregan^k, Roser Vilatersana^a, Juan Viruel^l, Bayram Yıldız^m, Frederik Leliaertⁿ, Alexey P. Seregin^o, Cristina Roquet^e

^a Botanic Institute of Barcelona (IBB), CSIC-CMCNB, Pg. Mígia, s.n., 08038 Barcelona, Spain

^b Department of Biology, Autonomous University of Madrid, Madrid, Spain

^c Department of Research & Conservation, Denver Botanic Gardens, Denver, CO 80206, USA

^d Department of Pharmaceutical Botany, Faculty of Pharmacy, İnönü University, Malatya, Türkiye

^e Autonomous University of Barcelona, Systematics and Evolution of Vascular Plants (UAB) – Associated Unit to CSIC by IBB – Cerdanyola del Vallès, Spain

^f Natural History Museum, University of Oslo, PO Box 1172 Blindern, NO-0318 Oslo, Norway

^g Department of Biology, Faculty of Necatibey Education, Balıkesir University, 10145 Balıkesir, Türkiye

^h Kochi Prefectural Makino Botanical Garden, 4200-6, Godaisan, Kochi 781-8125, Japan

ⁱ State Key Laboratory of Systematic and Evolutionary Botany, Institute of Botany, Chinese Academy of Sciences, 100093, Beijing, China

^j Department of Urban Greening and Vegetation Ecology, Norwegian Institute of Bioeconomy Research, Ås, Norway

^k Department of Biology, Science and Research Branch, Islamic Azad University, Tehran, Iran

^l Royal Botanic Gardens, Kew, Richmond, UK

^m Yenikale District, İsmail Cem Street, No. 35, Narlıdere, İzmir, Türkiye

ⁿ Meise Botanic Garden, Nieuwelaan 38, 1860 Meise, Belgium

^o Faculty of Biology, M. V. Lomonosov Moscow State University, Moscow, 119991, Russia

ARTICLE INFO

Keywords:

Biogeography
Carduinae
Cirsium
Diversification
Target-enrichment
Taxonomy

ABSTRACT

Widely distributed plant genera offer insights into biogeographic processes and biodiversity. The Carduus-Cirsium group, with over 600 species in eight genera, is diverse across the Holarctic regions, especially in the Mediterranean Basin, Southwest Asia, Japan, and North America. Despite this diversity, evolutionary and biogeographic processes within the group, particularly for the genus *Cirsium*, remain underexplored. This study examines the biogeographic history and diversification of the group, focusing on *Cirsium*, using the largest molecular dataset for the group (299 plants from 251 taxa). Phylogenomic analyses based on 350 nuclear loci, derived from target capture sequencing, revealed highly resolved and consistent phylogenetic trees, with some incongruences likely due to hybridization and incomplete lineage sorting. Ancestral range estimations suggest that the Carduus-Cirsium group originated during the Late Miocene in the Western Palearctic, particularly in the Mediterranean, Eastern Europe, or Southwest Asia. A key dispersal event to tropical eastern Africa around 10.7 million years ago led to the genera *Afrocarduus* and *Afrocirsium*, which later diversified in the Afrotropical region. The two subgenera of *Cirsium*—*Lophiolepis* and *Cirsium*—began diversifying around 7.2–7.3 million years ago in the Western Palearctic. During the Early Pliocene, diversification rates increased, with both subgenera dispersing to Southwest Asia, where extensive *in situ* diversification occurred. Rapid radiations in North America and Japan during the Pleistocene were triggered by jump-dispersals events from Asia, likely driven by geographic isolation and ecological specialization. This added further layers of complexity to the already challenging taxonomic classification of *Cirsium*.
Keywords: Biogeography; Carduinae; *Cirsium*; Diversification; North Hemisphere; Target-enrichment; Taxonomy.

* Corresponding author.

E-mail address: luciad.moreyra@ibb.csic.es (L.D. Moreyra).

<https://doi.org/10.1016/j.ympev.2025.108285>

Received 8 October 2024; Received in revised form 20 December 2024; Accepted 5 January 2025

Available online 10 January 2025

1055-7903/© 2025 Elsevier Inc. All rights are reserved, including those for text and data mining, AI training, and similar technologies.

1. Introduction

During the last decade, macroevolutionary, taxonomic, and biogeographic studies have strongly benefited from the advent of new molecular (e.g. Weitemier et al. 2014) and bioinformatic tools (e.g. Johnson et al. 2016). Such advances have significantly enhanced phylogenetic resolution, even in recently diverged and highly diversified plant lineages. This improvement has provided solid phylogenetic hypotheses essential for studies of diversification and biogeographic history, as well as for refining taxonomic classifications of complex groups (e.g. Mandel et al. 2019; Herrando-Moraira et al. 2019; Watson et al. 2020; Siniscalchi et al. 2021).

Widely distributed and highly diverse plant groups offer unique opportunities to investigate how biogeographic processes and past climatic/geological changes have shaped current biodiversity patterns at a global scale (e.g. Dupin et al., 2017; Gorospe et al., 2020), and to address the main drivers of diversification in species-rich regions (e.g. Herrando-Moraira et al. 2023). Subtribe Carduinae is an interesting group of plants for studying biogeography and diversification processes as it is one of the most speciose subtribes in tribe Cardueae, with ca. 600 species in 13 genera (Moreyra et al., 2023). The subtribe occurs predominantly in the Northern Hemisphere, with its highest diversity in the Mediterranean Region and South-West Asia (Herrando-Moraira et al., 2019; Ackerfield et al., 2020). The largest genus in this subtribe is *Cirsium* Mill. (ca. 420 species), which also is one of the largest genera in the Compositae. *Cirsium* is also the most taxonomically complex genus of the subtribe (Table 1). Its species have been classified into at least 16 different genera, and their demilitation is still under discussion (Ackerfield et al., 2020). Recently, *Cirsium* was split into four genera (Del Guacchio et al., 2022), but this was based on a poorly resolved phylogenetic tree based on two nuclear and five plastid markers. Here we follow the generic classification of the subtribe suggested in our recent phylogenomic study (Moreyra et al., 2023).

Within *Cirsium*, two subgenera are commonly recognized: *Lophiolepis* Cass. and *Cirsium* (Bureš et al., 2023). This classification reflects two groups of species that can be clearly distinguished by morphology (Bureš et al., 2023) and correspond to two distinct evolutionary lineages (Moreyra et al., 2023). The subgenera also differ in biogeographic range and ecological preferences: *Lophiolepis* occurs in the Palearctic region with mostly xerophilous species (Davis & Parris, 1975; Bureš et al., 2023), while *Cirsium* occurs in both the Palearctic and Nearctic regions,

with species in xeric as well as in mesic habitats such as alpine meadows or open forests in temperate climates (Bureš et al., 2023).

The geographic origins of *Cirsium* and its main lineages remain unknown. We also lack a biogeographic study based on a solid phylogenetic framework with a comprehensive taxonomic sampling to unravel the main processes that have driven its current widespread distribution in the Northern Hemisphere. Previous studies have mostly focused on the geographic origins of the North American radiation (Ackerfield et al., 2020; Siniscalchi et al., 2023). However, the highest diversity in both subgenera is found in South-West Asia (ca. 200 species), suggested to be the center of the origin of several Cardueae clades (Herrando-Moraira et al., 2019). Subgenus *Cirsium* is also highly diverse in North America, Japan, and the Western Mediterranean region (Werner et al., 1976; Talavera, 2015; Ackerfield et al., 2020), whereas *Lophiolepis* is highly diverse in the Eastern Mediterranean region (Charadze, 1963; Davis & Parris, 1975; Bureš et al., 2023). Given their differences in habitats and geographic range, it seems likely that the two subgenera differ in time of origin and diversification dynamics as well.

Here we investigate the evolutionary and biogeographic history of the genus *Cirsium* based on a robust phylogenetic framework, and in particular addressing the contentious issues regarding its generic boundaries. We first assembled a taxonomically and biogeographically comprehensive sample set of the entire Carduus-Cirsium group (Fig. 1) with a particular focus on *Cirsium*, including more than 60 % of its species. We obtained sequences of nuclear loci by applying the target enrichment approach with the Compositae1061 probe set (Mandel et al., 2014), and carefully assessed the orthology of the sequences. The resulting phylogeny was time-calibrated, and ancestral range inference based on a probabilistic approach (Matzke, 2013) was conducted to elucidate the biogeographic origins and history of the group. Finally, we investigated the diversification dynamics of *Cirsium* by fitting time-, environmental- and diversity-dependent models (Etienne et al., 2012; Morlon et al., 2016), as well as constant models, to test for different macroevolutionary scenarios.

2. Material and methods

2.1. Taxon sampling

We sampled 295 accessions of subtribe Carduinae (following Moreyra et al., 2023), including 266 samples of *Cirsium* (248 species; c. 60 % of the genus). For the other genera belonging to the Carduus-Cirsium group, we included eleven samples of *Carduus*, three of *Afrocarduus*, four of *Afrocirsium*, two of *Silybum*, one from the monotypic *Tyrinnus*, four of *Picnomon* and four of *Notobasis*. For the remainder of the subtribe, we included one species from each of the genera *Cynara*, *Ptilostemon*, *Lamyropsis* and *Galactites*, and two species of *Nuriaeae*. Four species of subtribe Onopordinae Garcia-Jacas & Susanna (sister to subtribe Carduinae) and one from Echinopsinae Cass. ex Dumort. were included as outgroup taxa following the classification of Herrando-Moraira et al. (2019). The sampling was designed to cover not only the main taxonomic groups but also the geographic distribution. A total of 188 samples were newly sequenced from fresh material collected in the field and preserved in silica-gel or from herbarium specimens from ARIZ, ASU, B, BC, BONN, BR, BRY, CS, JACA, MA, MADJ, MBK, MEXU, MW, OBI, PE, RENO, RM, RSA, TARI, TEX, T, TOKMM, USCH, RSA, RM, RJB, UNM, USCH, W, WAG and WTU (studied material in Table S1). The sequences of the 111 remaining samples were previously obtained by Moreyra et al. (2023). Detailed sample information and accession numbers are provided in Table S1.

2.2. DNA extraction and target-capture sequencing

For the new samples analyzed in this study, we performed target capture sequencing using the Compositae1061 kit (Daicel Arbor Biosciences, Ann Arbor, Michigan, USA: Mandel et al., 2014) following the

Table 1
Summary of the main taxonomic treatments of the relevant clades and species discussed in this study.

Study/Taxa	Eurasian + North American Clade	West Asia clade	<i>Cirsium vulgare</i> (Savi.) Ten.	<i>Cirsium italicum</i> DC.
De Candolle and Duby, 1828, De Candolle, 1837	<i>Cirsium</i> sect. <i>Cirsium</i>	<i>Cirsium</i> sect. <i>Epitrachys</i> DC.	<i>Cirsium</i> sect. <i>Epitrachys</i> DC.	<i>Cirsium</i> sect. <i>Epitrachys</i> DC.
Ackerfield et al., 2020	<i>Cirsium</i> Mill.	<i>Eriolepis</i> Cass.	<i>Eriolepis</i> Cass.	<i>Eriolepis</i> Cass.
Del Guacchio et al., 2022	<i>Cirsium</i> Mill.	<i>Lophiolepis</i> Cass.	<i>Cirsium</i> Mill.	<i>Epitrachys</i> (DC. ex Duby) K. Koch
Bureš et al., 2023	<i>Cirsium</i> subg. <i>Cirsium</i>	<i>Cirsium</i> subg. <i>Lophiolepis</i> Cass.	<i>Cirsium</i> subg. <i>Cirsium</i>	"italicum clade"
Moreyra et al., 2023	<i>Cirsium</i> sect. <i>Cirsium</i>	<i>Cirsium</i> sect. <i>Epitrachys</i> DC.	<i>Cirsium</i> sect. <i>Cirsium</i>	Not included
This study	<i>Cirsium</i> subg. <i>Cirsium</i>	<i>Cirsium</i> subg. <i>Lophiolepis</i> Cass.	<i>Cirsium</i> subg. <i>Cirsium</i>	<i>Cirsium</i> subg. <i>Cirsium</i>

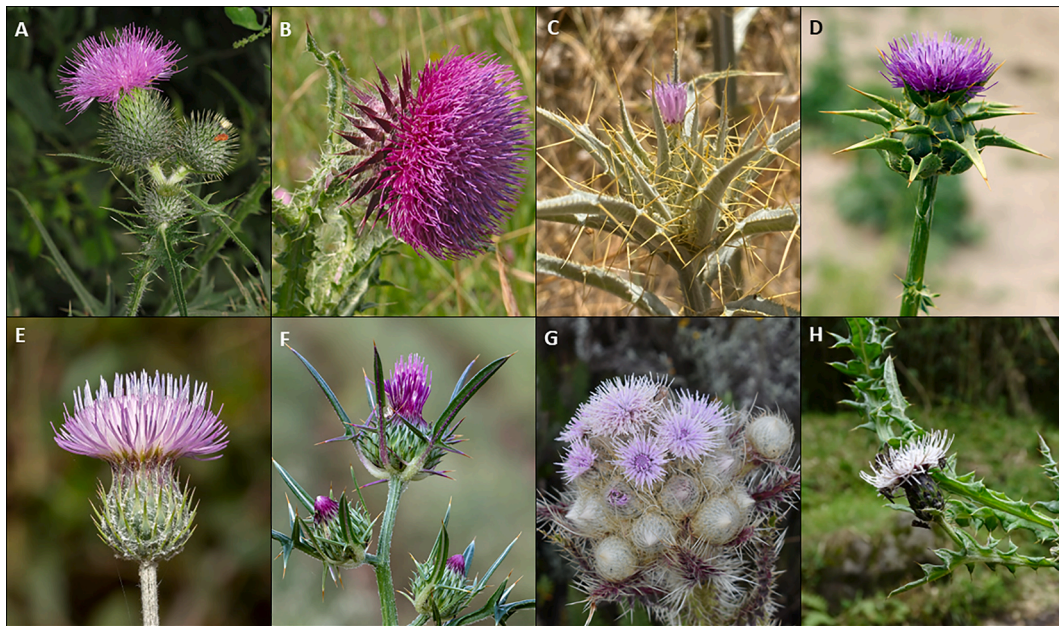


Fig. 1. Diversity of the *Carduus-Cirsium* group genera: (A) *Cirsium vulgare* (Savi) Ten., (B) *Carduus nutans* L., (C) *Picnomon acarna* (L.) Cass., (D) *Silybum marianum* (L.) Gaertn., (E) *Tyrimmus leucographus* (L.) Cass., (F) *Notobasis syriaca* (L.) Cass., (G) *Afrocarduus keniensis* (R.E.Fr.) Garcia-Jacas, Moreyra & Susanna, (H) *Afrocarduus buchwaldii* (O.Hoffm.) Calleja, Garcia-Jacas, Moreyra & Susanna. Photos A–F, under Creative Commons License: CC BY 4.0, CC BY-SA 4.0; authors: (A–B) Robert Flogaus-Faust, (C) Konstantinos Barsakis, (D) Krzysztof Ziarnik, (E) Eleftherios Katsillis, (F) Zeynel Cebeci. Photos G and H: Lucía D. Moreyra and Mercè Galbany-Casals, respectively.

same steps as detailed in Moreyra et al. (2023). First, 20–50 mg of dried plant material was measured per sample. DNA was extracted using E.N. Z.A® SP Plant DNA Kit (Omega Bio-Tek Inc., Norcross Georgia, USA) following the manufacturer's instructions. DNA concentration was calculated using Qubit™ 3.0 Fluorometer (Thermo Scientific, Waltham, MA, USA) and then sheared (100 ng–1 µg in 50 µl) using a Qsonica Q800R3 Sonicator (Qsonica LLC, Newtown CT, USA) at 20 % amplitude for 45 s to 20 min at 4 °C to obtain fragments of 300–400 bp. The length of the fragments was checked by electrophoresis in 1.2 % agarose gel.

Genomic libraries were prepared from 25–45 µl of sample using NEBNext Ultra II DNA Library Prep Kit for Illumina (New England Biolabs, Ipswich, Massachusetts, USA), using half of the volumes stipulated by the manufacturer and fifteen cycles of PCR amplification. Libraries were barcoded with dual index primers NEBNext® Multiplex Oligos for Illumina® or NEBNext Multiplex Oligos for Illumina (96 Index Primers) (New England Biolabs, Ipswich, Massachusetts, USA). Samples with less than 50 ng were discarded. Pools containing 10 genomic libraries were mixed in equimolar conditions. Subsequently, pools were evaporated or filled with water to 7 µl of volume to execute a target-enrichment protocol using the MyBaits Compositae-1061 kit. Pools were sequenced (150 bp PE) using HiSeq 2500 and HiSeq X by Macrogen Co. (Seoul, South Korea).

2.3. Raw sequence processing and nuclear ortholog assignment

Raw reads were trimmed using Trimmomatic v.0.32 (Bolger et al., 2014). After checking the quality of the reads using FastQC, quality-trimmed reads were assembled to contigs using BWA (Li & Durbin, 2009) as implemented in HybPiper (Johnson et al., 2016). As a reference file, we used the original Compositae-1061 target file plus the same exons recovered from the *Cirsium tioganum* sample, which we previously mapped using HybPiper and yielded the highest coverage in our data set (~50x). These sequences were added to the target file to account for sequence diversity and to improve loci retrieval during the mapping and assembly steps (McLay et al., 2021).

Due to the prevalence of polyploidy in Compositae (Moore-Pollard et al., 2024), paralogous sequences (hereafter paralogues) require

thorough investigation. To ensure that our final alignments only included orthologous sequences, we applied the following procedure: first, we assembled the genes mapping the new target file using HybPiper. Then, we filtered the genes taking into account the paralog warnings generated by HybPiper, discarding those genes with more than 10 paralog warnings. For the genes that had between 1 and 10 paralog warnings, we used the paralog retriever pipeline from HybPiper to also recover the potential paralogs. We aligned these sequences using MAFFT v.7.029 (Katoh & Toh, 2008) and trimmed using TrimAl (Capella-Gutiérrez et al., 2009), with the –all option to build gene trees using RAXML v.8.2 (Stamatakis, 2014). We visually inspected gene-tree topology and selected those genes in which the designation of the orthologous and paralog copy was made correctly, according to the phylogenetic position expected for that species based on the current phylogenetic knowledge of the study group (Ackerfield et al., 2020; Bureš et al., 2023; Moreyra et al., 2023). Genes with more than one paralog and misassigned orthologous sequences (i.e. assigned by HybPiper as paralogues instead of orthologous and vice versa) were discarded. Finally, genes that presented less than 50 % of missing data, and that included at least 80 % of species presence were retained. This type of approach has provided good results in phylogenetic studies avoiding the loss of a considerable proportion of potentially informative loci (Soto Gomez et al., 2019). After gene selection, we ran HybPiper using the –run_intronrate option to also recover introns and intergenic sequences flanking targeted exons. All matrices were aligned and trimmed as described above. The final dataset consisted of 350 alignments, which were concatenated to generate a supermatrix using FasnCAT-G v.1.05.1 (Kück & Longo, 2014).

2.4. Phylogenetic analyses

Concatenated and coalescence-based approaches were applied to infer the evolutionary history of the study group. For the concatenated approach, a partitioned analysis was run based on the 350-gene supermatrix, using RAXML-NG-MPI (Kozlov et al., 2019) in CESA cluster (Galicia Center for Supercomputing Technology, Santiago de Compostela, Spain). For each locus, the best-fit evolutionary model was selected

using ModelTest-NG (Darrriba et al., 2019). A total of 250 independent searches were done to search for the best tree. Branch support analyses were run using the autoMRE option, which generates bootstrap trees until these converge; branch support was calculated both using Felsenstein's Bootstrap (BS) and Transfer Expectation Bootstrap (TBE).

For the coalescence analysis, gene trees were calculated using RAXML-NG in CESGA and the analysis was done using ASTRAL-III v.5.7.8 (Zhang et al., 2018) as implemented in the HybPhyloMaker pipeline (Fér & Schmickl, 2018). Support values were calculated using local posterior probabilities (LPP), and branches were considered to be supported when LPP was ≥ 0.95 . To detect the degree of incongruence between gene trees, a quartet-based method analysis was run with the -t 8 option of ASTRAL-III, which allows for identifying the percentage of genes that support alternative topologies for each node.

2.5. Divergence time estimation

We used the RelTime method (Tamura et al., 2012; Tamura et al., 2018; Tao et al., 2020) implemented in MEGA X (Kumar et al., 2018) to generate a time-calibrated phylogeny, using as input the best Maximum Likelihood tree obtained from the concatenated analysis. Three calibration points were included to constrain nodes (Fig. S3). The mean age for the root (CP1, Fig. S3) was set at 17.7 Mya (based on Mandel et al., 2019) with a normal distribution and a softbound in which the lower limit corresponded to 14 Mya, because there is fossil evidence of achenes similar to those found in *Afrocarduus*, *Afrocirsium*, *Cirsium* and *Nuriaeae* (Mai, 1995). The upper bound was the result of setting a normal distribution for the mean of 17.7 Mya and the lower bound of 14 Mya. The other two calibration points were the following: we set a minimum age of 14 Mya to CP2 (Fig. S3) based on a fossil Cirsioide achene (Mai, 1995), and we set a maximum age of 5.6 Mya to CP3 (Fig. S3) for the most recent common ancestor of the populations sampled for *Cirsium latifolium*, which is endemic to Madeira, based on the estimated geological age of this archipelago (Ramalho et al., 2015).

2.6. Historical biogeographic inference

We focused the biogeographic analyses on the *Carduus-Cirsium* group, trimming from the calibrated tree the outgroup and the genera *Cynara*, *Galactites*, *Lamyropsis*, *Nuriaeae* and *Psilostemon*. We also left only one tip for each taxon when multiple individuals were sequenced. Moreover, we followed the suggestion by Bureš et al. (2023) to exclude *Cirsium italicum*, as its position in the tree was very different from the one retrieved in the coalescent tree.

We collected information on the distribution area for each species from floras and online resources (Charadze, 1963; Davis & Parris, 1975; Werner et al., 1976; Petrak, 1979; Shi et al., 2011; Iwatsuki et al., 1995; Talavera, 2015; POWO: <https://powo.science.keew.org>), and also from voucher herbarium specimens (see Table S1). The geographic areas were defined taking into account the main distribution of endemic species and the main biogeographic regions of the world. A total of 13 operational areas were defined (Fig. 2) to cover the distribution of the species from the subtribe. These include four areas in America: Southern North America (J), Western North America (K), Eastern North America (L), Central North America (M); three in Africa: North Africa (G), Macaronesian archipelagos (H), Afromontane region (I); and six in Eurasia: Middle Asia (A), East Asia (B), South-West Asia (C), Japan (D), Euro-Siberian Region (E), North Mediterranean Basin (F).

We estimated geographic range evolution using the R package BioGeoBEARS v.1.1.3 (Matzke, 2013; available at <https://github.com/nmatzke/BioGeoBEARS>). We set the maximum number of areas allowed in each node to five, which is the number of areas that occupy the most widespread species of our phylogeny (*Cirsium vulgare*), to make the analysis computationally feasible.

We evaluated the adequacy of three biogeographic models: 1) the dispersal-extinction-cladogenesis model (DEC; Ree et al., 2005; Ree & Smith, 2008), 2) a likelihood-based implementation of the dispersal-vicariance analysis model (DIVALike; Ronquist, 1997), and 3) a version of the BAYAREA model (BAYAREALike; Landis et al., 2013), which assumes that range evolution does not occur at cladogenetic events. Furthermore, we fitted a more complex version of each model adding the jump-dispersal parameter (DEC + j, DIVALike + j,

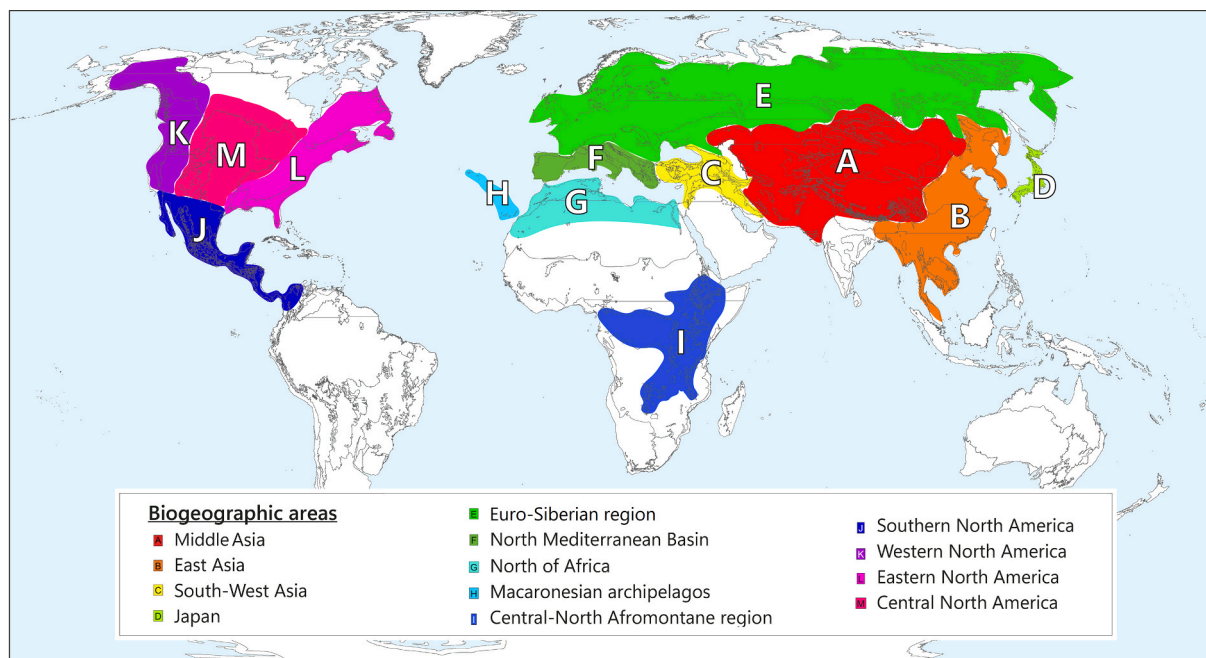


Fig. 2. Geographic representation of the 13 geographic areas defined in the current study: Middle Asia (A), East Asia (B), South-West Asia (C), Japan (D), Euro-Siberian Region (E), North Mediterranean Basin (F), North Africa (G), Macaronesia (H), Central-North Afromontane Region (I), Southern North America (J), Western North America (K), Eastern North America (L), Central North America (M).

BAYAREALike + j; Matzke, 2014) to account for founder-event speciation. This parameter represents a range jump occurring during lineage-splitting events, where one daughter lineage occupies a new range while the other retains the ancestral range (Matzke, 2014). The evaluation of the best-fitting model was based on the Akaike Information Criterion (AIC) and AIC weights (AICwt) (Burnham & Anderson, 1998). Additionally, we employed Biogeographic Stochastic Mapping (BSM) analysis (Dupin et al., 2017) with 100 replicates to determine the average occurrences of anagenetic and cladogenetic events considering geographic distributions, phylogeny, and the best-fitting model.

2.7. Diversification analyses

As a preliminary analysis, we outlined the progression of lineages over time using a lineage-through-time plot (LTT; Nee et al., 1992). To accomplish this, we used the R package *ape* and the *mltt.plot* function (Paradis & Schliep, 2019), with the y-axis representing the number of lineages in a logarithmic scale. We examined the diversification dynamics of *Cirsium* using a hypothesis-driven methodology to sidestep identifiability issues, as recommended by Louca & Pennell (2020) and Morlon et al. (2022). In essence, we defined diversification models to test whether speciation or extinction rates varied linearly or exponentially with time or climate changes (global temperature variation; Zachos et al., 2008). We also fitted two constant-rate models (pure-birth and birth–death) as null hypotheses. These analyses were implemented using the R package *RPANDA* (Morlon et al., 2016). We also tested whether the rate of species diversification was dependent on species diversity, fitting (1) models in which the carrying capacity, i.e. the number of species that can exist at the same time, represented by the parameter (*K*), was the same for the entire study group; and (2) models in which all parameters were allowed to shift at a certain time (parameter *t*_shift), to test whether there was a significant shift in diversification dynamics during the history of *Cirsium*, as the visual inspection of the LTT plot suggested. These last models were run using the R package *DDD* (Etienne et al., 2012). We applied to all models an analytical correction corresponding to the sampling fraction to account for incomplete taxon sampling. All models were compared based on AIC and the most fitted model was identified as the one with the minimal AIC value.

3. Results

3.1. Target loci recovery

Of the 1,064 loci originally mapped from the target reference, we retained 350 (for more information about paralogs detected, sequence lengths, and statistics reports, see Table S2). Because we used the “supercontig” option on HybPiper, the average length of each alignment was more than twice the length of the original reference. In combination, the 350 genes accounted for 158,591 parsimony informative sites and 251,647 patterns (unique columns in the alignment). The nuclear supermatrix generated for the concatenated analysis had a length of 319,583 bp. For the coalescence analysis, a gene tree was calculated for each of the 350 alignments.

3.2. Phylogenetic Relationships

The concatenated and coalescence analyses yielded similar topologies (Figs. S1 and S2) except for a few nodes. The percentages of supported nodes (≥ 70 % of BS or TBE, and ≥ 0.95 of LPP) for the concatenated analyses were 83 % (TBE) and 69 % (BS); for the coalescence analysis, it was 68 % (LPP). The genera *Cynara*, *Galactites*, *Lamyropsis* and *Nuriaeae* were recovered outside the *Carduus*–*Cirsium* group in both phylogenies, with high support (BS = 100; TBE = 1; LPP = 1). Within the *Carduus*–*Cirsium* group, the genus *Carduus* was fully supported as monophyletic (BS = 100; TBE = 1; LPP = 1) with

Tyrminnus as sister (BS = 100; TBE = 1; LPP = 1), and with *Silybum* as sister to *Carduus* + *Tyrminnus* clade (BS = 100; TBE = 1; LPP = 1). The monotypic genus *Picnomon* was recovered as sister to the monotypic *Notobasis* (BS = 70; TBE = 0.82) in the concatenated analysis, whereas in the coalescence approach, it was recovered as sister to *Cirsium* subg. *Lophiolepis* with high support (LPP = 1). In consequence, the genus *Cirsium* was recovered as monophyletic in the concatenated analyses (TBE = 0.89), whereas in the coalescence analysis, *Picnomon* was included in *Cirsium* with high support (LPP = 1). Within *Cirsium*, the main topological difference between two analyses was due to *Cirsium italicum*. In the coalescence tree, each of the subgenera *Cirsium* and *Lophiolepis* were monophyletic with high support (LPP = 1 and 0.95, respectively). In the concatenation phylogeny, however, *C. italicum* was recovered as sister to all other *Cirsium* species (TBE = 0.89).

3.3. Divergence times and ancestral ranges

The stem age of the *Carduus*–*Cirsium* group was estimated to 16.3 Mya, and it started to diversify at 11.3 Mya (9.1–13.8 95 % CI, Fig. S3). The stem and crown ages of *Cirsium* were 10 and 9.5 Mya (7.2–12.2 Mya 95 % CI), respectively, and the subgenera diverged at 8.8 Mya and started to diversify at similar times (7.2–7.3 Mya; 5.2–10 and 5.5–9.7 Mya 95 % CI, respectively).

The BAYAREALike + j model was selected as best-fitting (AICwt = 1, Table S3). Range contraction (*e* = 0.0499) had a much larger contribution than range expansion by dispersal (*d* = 0.0068) and founder event speciation processes (*j* = 0.0069). A considerable number of the ancestral ranges inferred for deep and intermediate nodes involved two or more areas, consistent with the high level of range contraction. For the deepest nodes, we obtained a high number of possible states with low probabilities; however, at least 90 % of the probability always included four areas: South-West Asia (C; hereafter SW Asia), the Euro-Siberian region (E), the North Mediterranean Basin (F; hereafter N Mediterranean Basin) and North Africa (G).

The most probable ancestral range of *Cirsium* (node 1, 8.8 Mya, 6.7–11.5 Mya 95 % CI, Fig. 3) involved four areas: SW Asia (C), the North Mediterranean Basin (F), the Euro-Siberian region (E) and North Africa (G). The ancestral range of the lineage formed by most species of subg. *Lophiolepis* (node 2, 7.2 Mya, 5.2–10 Mya 95 % CI) involved the N Mediterranean Basin (F) and North Africa (G) with 50 % probability, and the rest of the probability was shared among different combinations of the following areas: N Mediterranean Basin (F), Euro-Siberian region (E), North Africa (G), and SW Asia (C). The two following divergence events yielded two lineages mainly distributed in N Mediterranean Basin (F) and/or North of Africa (G). A jump dispersal towards SW Asia (C; node 5, 4.8 Mya, 3.3–6.9 Mya 95 % CI) was followed by extensive *in situ* diversification plus additional jump dispersals to Middle Asia (A) and more recently to the N Mediterranean Basin (F). The second dispersal to N Mediterranean Basin (F; node 6, 0.66 Mya, 0.5–1.8 Mya 95 % CI) was followed by notable diversification; in addition, at least two back dispersals occurred to SW Asia (C), and two lineages dispersed or expanded their range to the Euro-Siberian region (E).

The ancestral range of subg. *Cirsium* (node 7, 7.3 Mya, 5.5–9.7 Mya 95 % CI) had highest probability (40 %) in the North Mediterranean Basin (F), Euro-Siberian region (E) and North Africa (G). The first divergence event resulted in one small lineage (node 8, 5.1 Mya, 3.6–7.1 Mya 95 % CI, Fig. 3) originating from a jump to East Asia (B) or Middle Asia (A)/East Asia (B), and one large lineage (node 9, 6.4 Mya, 4.7–8.6 Mya 95 % CI) originating in the Euro-Siberian region (E) and the North Mediterranean Basin (F). Within the large lineage, several jump dispersals were inferred, including one to SW Asia (C) (node 10, 3.6 Mya, 2.5–5 Mya 95 % CI) and several to Middle Asia (A) and/or E Asia (B)/Euro-Siberian region (E)/N Mediterranean Basin (F). The sister clade of the lineage that originated from a jump dispersal to SW Asia (C; node 11, 3.8 Mya, 2.6–5.3 Mya 95 % CI) was formed by several lineages that remained in the ancestral range, with expansions to Middle Asia (A),

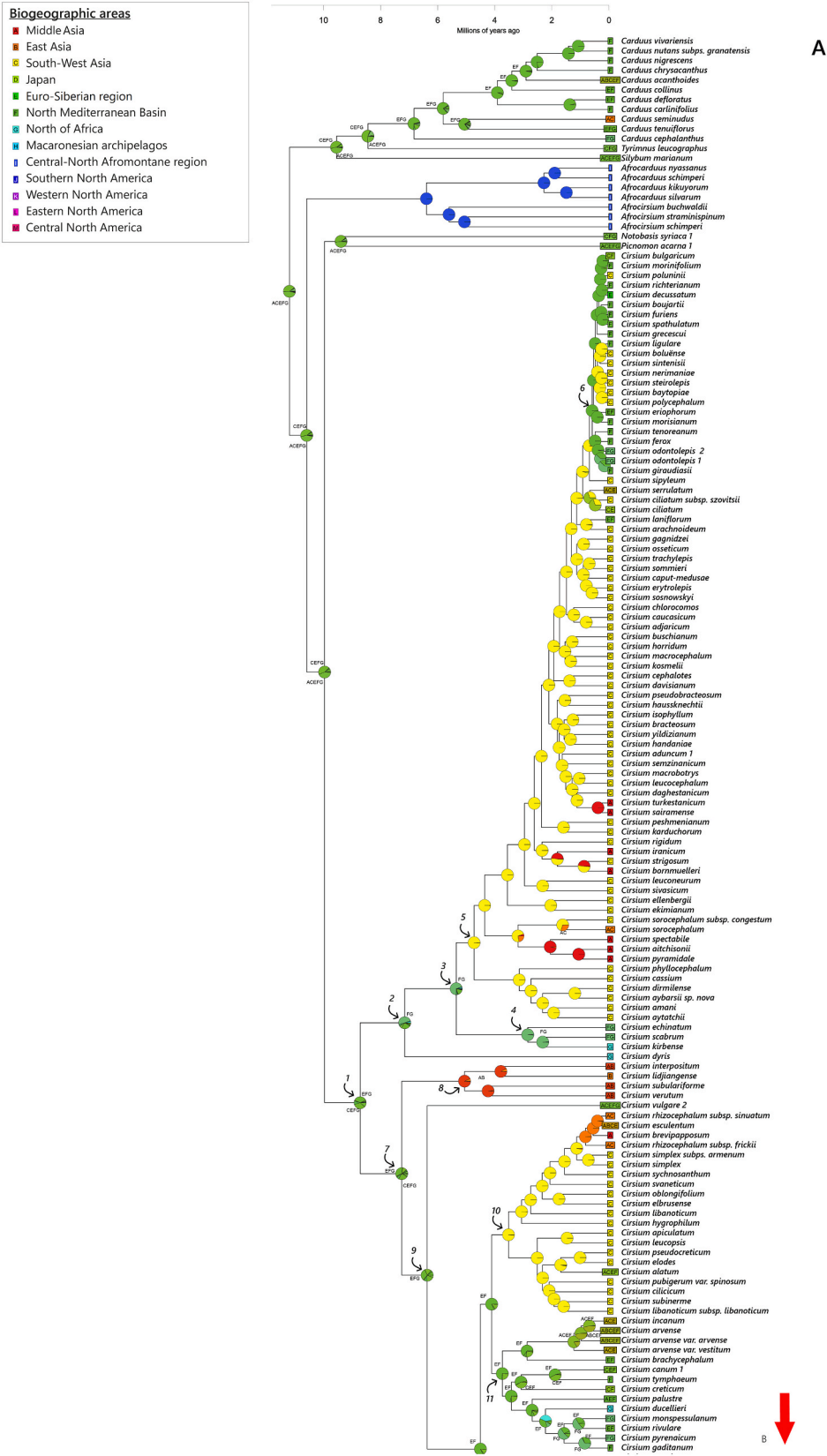


Fig. 3. Ancestral range estimation of the *Carduus*-*Cirsium* group using the best-fitting model BAYAREALIKE + j based on a time-calibrated phylogeny generated under the concatenation approach using target-enrichment data (Compositae1061 probe set). Pie charts at nodes show the relative probability of the possible states combining colors for more than one area. Node numbers are provided for nodes mentioned in the text.

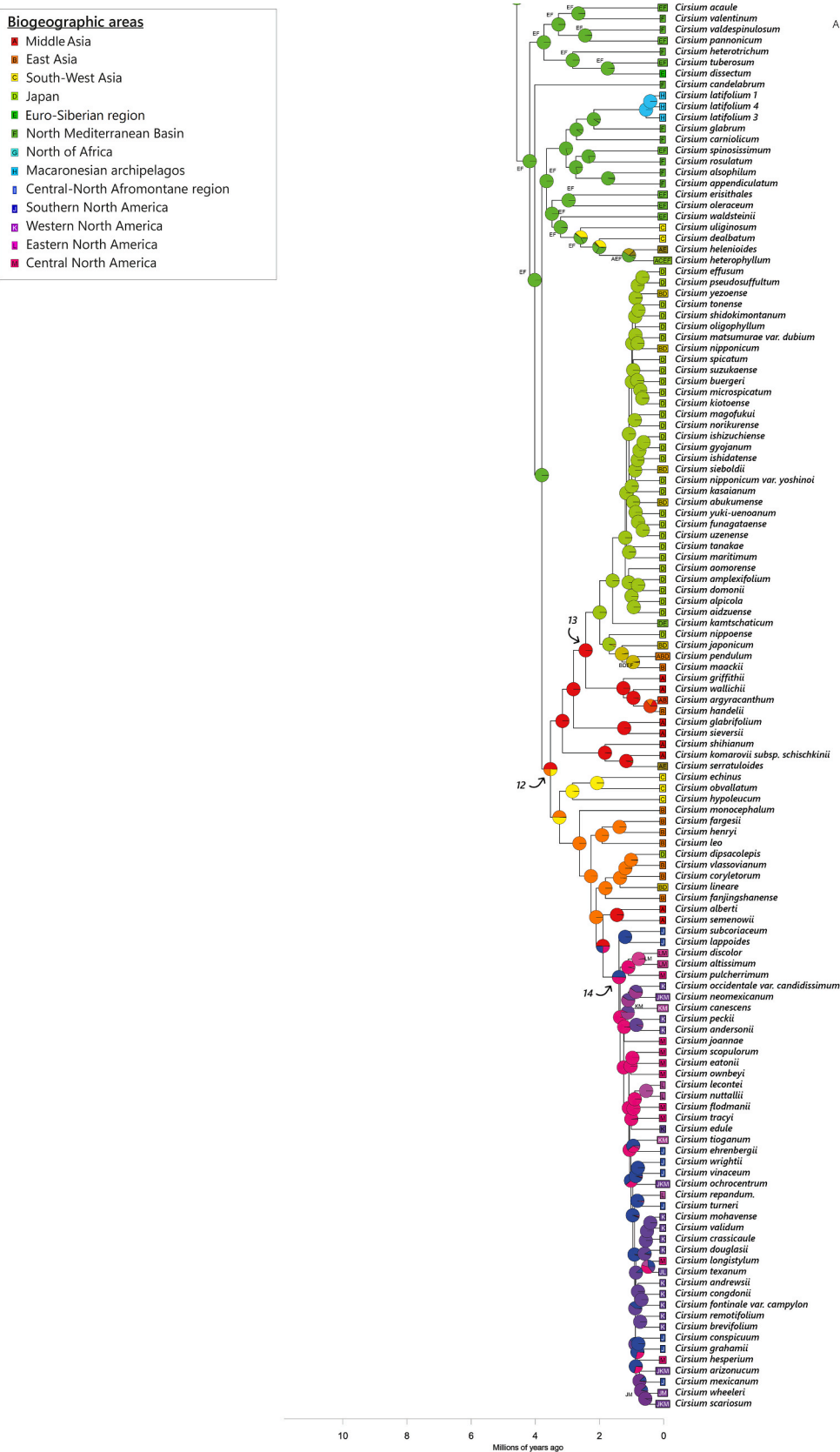


Fig. 3. (continued).

East Asia (B) and SW Asia (C). Another lineage descending from node 9 jumped to Asia (node 12, 3.5 Mya, 2.3–5.3 Mya 95 % CI). Later, one of the Asian lineages jumped to Japan (D; node 13, 2.4 Mya, 1.7–3.6 Mya

95 % CI) and another jumped to North America (node 14, 1.3 Mya, 0.7–2.5 Mya 95 % CI), both followed by rapid and notable diversification. Another jump dispersal to Japan (c. 1 Mya, 0.4–2.2 Mya 95 % CI)

resulted in the endemic *C. dipsacolepis*. Moreover, the ancestor of *C. lineare* originated from an ancestor that expanded its range from East Asia (B) to Japan (D) c. 1.4 Mya (0.7–2.7 Mya 95 % CI). One of the latest jump dispersals occurred from the N Mediterranean Basin (F) to Macaronesia (H; 0.54 Mya, 0.2–1.2 Mya 95 % CI) and resulted in *C. latifolium*, endemic to Madeira.

According to BSM analysis, the most frequent biogeographic events were within-area speciation (71 %), range expansion (18 %) and founder events (11 %) (Fig. 4; Tables 2 and Table S4). SW Asia (C) and the N Mediterranean Basin (F) played a key role in the diversification of the *Carduus-Cirsium* group as the majority of dispersal events occurred from or to one of these two regions (Fig. 4, Table S4). The most common dispersal patterns involved range expansions or jump dispersals from West to East: SW Asia (C) to Middle Asia (A) (8.4 events), and from the Mediterranean (F) to SW Asia (C) (6.8 events). The N Mediterranean Basin (F) was the source area of most dispersals (20 %), followed by West Asia (C; 18 %). The main sink area was Middle Asia (A; 20 %, Table S4). The Euro-Siberian region (E) was acting both as sink and source (11 % in both directions).

Dispersals towards Japan (D) occurred from Middle (A) and East Asia (B) (1.03 and 2.05 events, respectively), with several back-dispersals to East Asia (B; 5.04 events). American taxa originated from a single dispersal from Middle (A) or East Asia (B) (0.66 and 0.59 events). The Macaronesian (H) and North African (G) species originated from the N Mediterranean Basin (F) (1.1 and 2.6 events, respectively). The afro-montane lineages may have originated from the N Mediterranean Basin (F), SW Asia (C), North Africa (G) or the Euro-Siberian region (E; 0.29, 0.3, 0.23, 0.27 events, respectively).

3.4. Diversification analyses

We tested 24 different models: two constant-rate, six time-dependent, six temperature-dependent, six temperature–time dependent and four diversity-dependent models (Table S5). The best-fitted model was the diversity-dependent one with a time shift at 4.6 Mya and without extinction (AICc = 723.2; λ before shift = 0.44; λ after shift = 1.19; Fig. 5). The Δ AICc with the following best-fitted model

Table 2
Summary of biogeographic stochastic mapping counts for the *Carduus-Cirsium* group using the BAYAREALIKE + j model. Mean numbers of the different types of events estimated are shown along with standard deviations.

Mode	Parameter	Type	Mean (SD)	%
Within-area speciation Dispersal	y	Sympatry	235.9 (1.68)	71.0
	j	Founder	37.09 (1.68)	11.2
	d	Range expansion	59.12 (3.5)	17.8
	e	Range contraction	0 (0)	0.0
Total			332.1 (3.5)	100.0

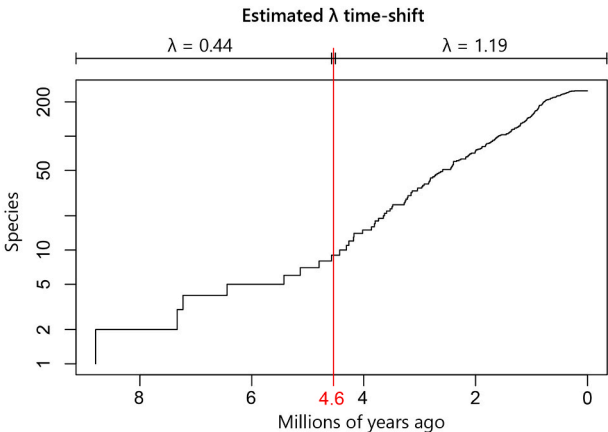


Fig. 5. Lineage-through-time plot (LTT) indicating the number of lineages that emerged (species; log-transformed) in a temporal line (Millions of years ago). Red line indicates the estimated time when the λ picked up from 0.44 to 1.19 according to the best-fitting diversification model.

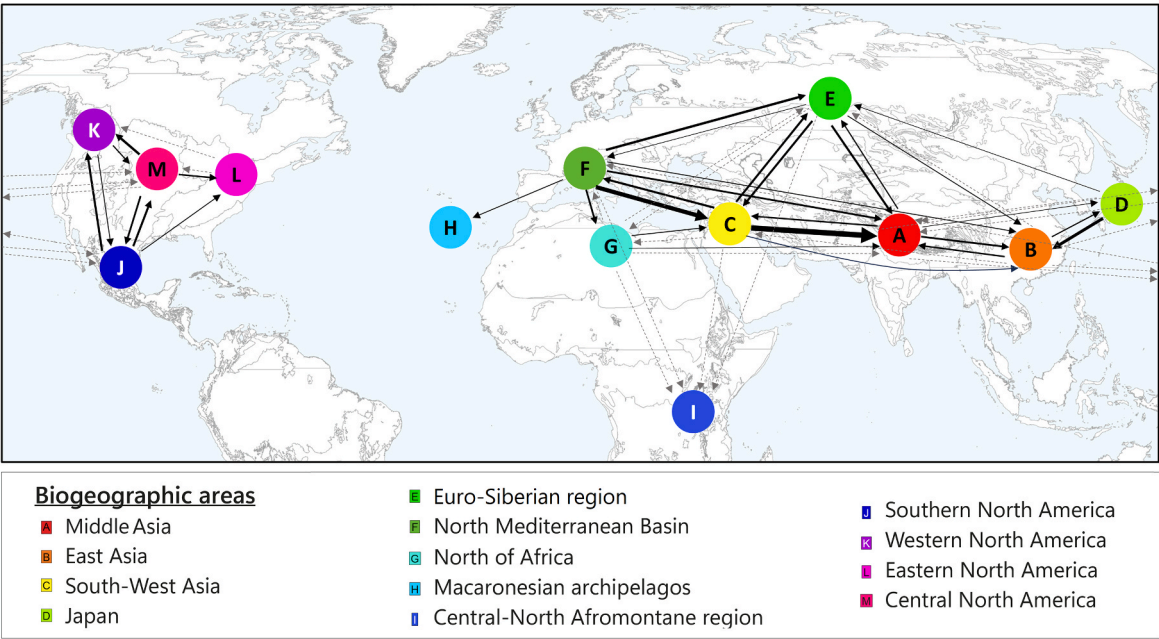


Fig. 4. Summary of mean dispersal events estimated from 100 biogeographic stochastic mappings in the *Carduus-Cirsium* group (see all event counts in Table 3). Whole arrows represent the mean number of dispersals > 0.95 with thickness proportional to the mean number of dispersals. The dotted arrows represent mean dispersals 0.20–0.94.

(diversity-dependent with time shift and extinction; AICc = 725.2) was equal to 2. Since the only difference between the first and the second best-fitted model is that the second one accounts for extinction, and the best-fitted model has two parameters less than the second best-fitted model, we will only discuss our results based on the first-fitted model. For the rest of the models $\Delta\text{AICc} > 25$.

4. Discussion

This study presents the first biogeographic analysis of *Cirsium* based on a highly resolved phylogeny and a broad and representative taxonomic sampling of the entire genus (266 samples, 248 species), made possible through a target-capture approach in combination with the careful application of up-to-date bioinformatic methods to assess sequence orthology. Our analysis incorporated 350 nuclear loci, more than 300,000 sites, and a quarter-million patterns (unique columns). In comparison, the most extensive previous phylogenetic study of *Cirsium* was based on 176 samples and seven molecular markers (Del Guacchio et al., 2022). Notably, our concatenated and coalescent-based phylogenetic approximations yielded well-resolved and largely congruent phylogenies, with discrepancies observed at only a few nodes. These few incongruencies are likely due to hybridization, a common phenomenon in this genus, as well as incomplete lineage sorting, typical of recent radiations (Ackerfield et al., 2020; Moreyra et al., 2023).

4.1. The early history of the *Carduus-Cirsium* group

We estimated that the ancestor of the *Carduus-Cirsium* group started to diverge at the beginning of the Late Miocene (11.3 Mya, 9.1–13.8 95 % CI; Fig. 3), a period marked by a global cooling trend (Westerhold et al., 2020), most likely in the regions surrounding the Mediterranean Sea, SW Asia or the Euro-Siberian region. This ancestor split into two lineages. One of these lineages includes the small genera *Silybum* and *Tyrimnus* plus *Carduus*, which has the highest species concentration in the Mediterranean Basin and South-West Asia. This lineage will not be further discussed here as it is not the main focus of the study.

The ancestor of the other lineage was distributed in the same range as its previous ancestor and lineage divergence started at 10.7 Mya (8.6–13.2 95 % CI). This timing coincides with a complex geological period that led to the formation of what is now the Mediterranean Region, transitioning from the open basin of Mediterranean Tethys to the modern closed basin with the closure of Paratethys (Cornacchia et al., 2018). This paleogeographic reorganization led to increased land connectivity between SW Asia and Northeast Africa, and may have facilitated the southward dispersal of one of the two descending lineages towards the mountains of tropical eastern Africa. This East African ancestor split into two lineages that correspond to the endemic genera *Afrocarduus* and *Afrocirsium*. *Afrocarduus* and *Afrocirsium* include species that were traditionally ascribed to *Carduus* and *Cirsium*, but we have recently shown that they constitute two independent evolutionary lineages with distinct sets of morphological features that can be morphologically distinguished from the other genera of the *Carduus-Cirsium* group (Moreyra et al., 2023).

The dispersal to montane and alpine habitats of tropical eastern Africa from the Mediterranean basin and western Asia may have been facilitated by the subtropical climate in mountainous environments in the source region during the Miocene (Pignatti, 1978; Kovar-Eder et al., 2006); this climate and the associated laurel evergreen forests later disappeared from the Mediterranean basin and western Asia. *Afrocarduus* and *Afrocirsium* currently occur in the montane and alpine temperate habitats that constitute the Afromontane region, which are markedly cooler and more humid than the surrounding arid lowlands (Gehrke & Linder, 2014). Thus, the ancestor of these genera could have been linked to the paleotropical flora that inhabited the northern hemisphere during the Tertiary. A few studies focusing on other plant groups have also reported that Tertiary lineages that went extinct in the

Mediterranean basin and/or in western Asia survived in the evergreen forests in the Afromontane Region (Mairal et al., 2015) or the oceanic islands of Macaronesia (Fernández-Palacios et al., 2011).

It is also interesting to note that the current species diversity in *Afrocarduus* and *Afrocirsium* mainly resulted from diversification during the Pliocene and Pleistocene, although their ancestor arrived much earlier (10.7 Mya, 8.6–13.2 95 % CI). Their diversification may have been fostered by the interplay of orogenic events and the intensification of global cooling since the Pliocene (Westerhold et al., 2020). High mountains existed in eastern Africa already during the Oligocene, but major uplift events still occurred during the Pliocene and Pleistocene (Sepulchre et al., 2006). Such orogenic activity, combined with the intensified global cooling, probably increased the total area of Afromontane and Afroalpine habitats in comparison to the Miocene (Gehrke and Linder, 2014).

The ancestor of the lineage containing the remaining genera, *Cirsium*, *Notobasis* and *Picnomon*, dates back to the late Miocene (10 Mya, 7.9–12.6 95 % CI) and probably occurred in the N Mediterranean Basin, N Africa, SW Asia and the Euro-Siberian Region. The monotypic genera *Notobasis* and *Picnomon* constitute the sister lineage of *Cirsium*, and they diverged from each other c. 9.5 Mya (7.3–12.3 95 % CI). These genera apparently persisted in the ancestral areas. However, this result should be taken with caution since our coalescence analysis shows the genus *Picnomon* as sister to subg. *Lophiolepis* (Figs. S1 and S2). This incongruence between the concatenated and coalescence approach was also observed in our previous study of subtribe Carduinae, and we hypothesized that it resulted from hybridization and incomplete lineage sorting (Moreyra et al., 2023).

The origin of *Cirsium* was also placed during the late Miocene, about 9 Mya (7.3–12.2 95 % CI), when a global cooling trend was happening (Herbert et al., 2016). This mean age is younger than that inferred by Ackerfield et al. (2020; 12 Mya). However, in their study, *Cirsium* was inferred as paraphyletic based on insufficiently informative loci, and this may have biased the dating analysis. Moreover, Ackerfield et al. (2020) placed the calibration point based on a fossil record of a Cirsioideae achene (Mai, 1995) at the *Carduus-Cirsium* group node, whereas we placed it at the node splitting the genus *Nuriaea* (recently described in Moreyra et al., 2023) from the remainder of the *Carduus-Cirsium* group (CP2, Fig. S3). Thus, Ackerfield et al. (2020) put this calibration point more closely to the present due to the lack of *Nuriaea* representatives in their phylogeny, and this could have pushed back the dating of the whole group.

4.2. Biogeographic history of *Cirsium*

The two main *Cirsium* clades, corresponding to the subgenera *Lophiolepis* and *Cirsium*, likely originated in the western Palearctic. Both lineages started to diversify at the end of the Miocene (7.2 and 7.3 Mya; 5.2–10 and 5.5–9.7 Mya 95 % CI, respectively), a period marked by accelerated global cooling and the onset of modern climatic conditions (Herbert et al., 2016). This period was characterized by global biotic turnovers (Herbert et al., 2016), and the Mediterranean Basin, one of the ancestral areas shared by the subgenera, is believed to have been at its driest during the latest Miocene, (6.6–5.3 Mya; Eronen et al., 2009). The speciation rate of *Cirsium* increased drastically during the Early Pliocene (4.6 Mya), almost tripling, from $\lambda = 0.44$ to $\lambda = 1.19$. The inferred time for the diversification rate shift coincides with two parallel dispersals (one in each subgenus, nodes 5 and 10, Fig. 3) towards SW Asia, one of the regions with the highest concentration of *Cirsium* species. Both dispersals were followed by substantial *in situ* diversification that lasted until the Late Pleistocene.

In subgenus *Lophiolepis*, the majority of the species are indeed found in SW Asia, although several dispersals to neighboring regions (Middle Asia, Euro-Siberian and Mediterranean region) occurred during the Pleistocene. One recent dispersal towards the N Mediterranean Basin (0.7 Mya; 0.5–1.8 Mya 95 % CI) was followed by a rapid radiation, and

also led to two back-dispersals to SW Asia. Because the vast majority of the species of this subgenus are adapted to the same type of habitats, allopatric processes may have prevailed in its diversification. The complex topography of SW Asia and the Mediterranean region, in combination with range contraction–expansion cycles due to Pleistocene climatic oscillations, probably fostered rapid non-adaptive radiations as reported for other plant genera such as *Dianthus* (Valente et al., 2010).

Subgenus *Cirsium* has a much wider geographic distribution than *Lophiolepis*. In addition to the regions where *Lophiolepis* is found, taxa of subgenus *Cirsium* also occur in East Asia, Japan, North America, and Macaronesia. This subgenus includes both mesophilous and xerophilous species (Bureš et al., 2023). The inferred ancestral range of subgenus *Cirsium* is the same as for *Lophiolepis*, but substantial diversification in subgenus *Cirsium* also occurred in the western Palearctic in parallel to the SW Asian diversification during the Pliocene and Pleistocene. The Eastern Mediterranean Region was a humid refugium for the Central European flora during the Early Pliocene, when the precipitation decreased in Central Europe (Eronen et al., 2009 and references therein). At the same time, the Asian Monsoon became weaker and xerophilous plants increased in Middle Asia (Zhao et al., 2020).

One of the western Palearctic ancestors of subgenus *Cirsium* dispersed to Middle Asia (node 12, Fig. 3) during the mid-Pliocene (3.8 Mya; 2.3–5.3 Mya 95 % CI) and split into two speciose Asian lineages. Each lineage dispersed to new areas and radiated rapidly there: one in Japan, and one in North America (further discussed below). The higher climatic niche lability of subgenus *Cirsium* (compared to subgenus *Lophiolepis*) may have fostered its geographic expansion to other regions. For instance, the dispersal to Middle Asia may have been associated with a change of habitat; most Middle Asian species are adapted to moist habitats such as riverbanks, gorges, forests, and montane slopes in montane or sub-alpine zones (Shi et al., 2011), and some species are generalists found across Central, East Asia and Japan (*C. maackii*, *C. pendulum*, and *C. japonicum*).

4.3. Rapid radiation of *Cirsium* in Japan

The Japanese archipelago harbors more than 100 *Cirsium* species, and the vast majority (90 %) are endemic (Iwatsuki et al., 1995). Whereas a previous biogeographic analysis included only three of them (Ackerfield et al., 2020), we here included 38 Japanese species (30 endemic). All but two of these species form a clade that originated from a single jump dispersal from Middle Asia to Japan at the beginning of the Pleistocene (c. 2.4 Mya; 1.7–3.6 Mya 95 % CI). Although our sampling is not complete, our results suggest that the high concentration of *Cirsium* endemics in Japan is mostly the result of a single rapid radiation following a dispersal event from the continent, a common pattern in islands. We hypothesize that this rapid radiation may result from an interplay of allopatric and ecological speciation, as reported for other rapid insular radiations in Cardueae (Vitales et al., 2014). Allopatry may have played an important role during the Pleistocene sea-level fluctuations, which resulted in varying connectivity among the Japanese islands (Pillans et al., 1998; Davison et al., 2005). Some species may have originated by ecological speciation linked to habitat specialization, such as *C. tamastoloniferum*, a narrow endemic living only in marshy lands (Kadota, 2012). A potential additional factor is polyploidy, however, the ploidy levels of only a few *Cirsium* species from Japan have been studied to date, including only four of our species; indeed, the frequency of polyploidy has not been extensively studied in *Cirsium*, but current knowledge suggest that this phenomenon is rare in its subtribe (Bureš et al., 2023).

4.4. The North American *Cirsium* radiation resulted from a single dispersal from Asia

Colonization of America from Asia is observed in many plant groups

(e.g., Nazaire et al., 2014; Wen et al., 2016), including thistles (Susanna et al., 2011). Previous studies (Kelch & Baldwin, 2003; Barres et al., 2013; Ackerfield et al., 2020) suggested that all American *Cirsium* species could result from a single dispersal event from Asia through the Bering Land Bridge during the Miocene (Ackerfield et al., 2020) or Pliocene (Barres et al., 2013). Our results confirm this single dispersal hypothesis, but we found that it took place from Central or East Asia during the Pleistocene (1.9 Mya; 0.7–2.5 Mya). A similar age was obtained by Siniscalchi et al., 2023 (2 Mya), whose study solely focused on North American *Cirsium* species. However, they suggested that diversification of this clade occurred 1.9–1.2 Mya, whereas our results suggest 1.3–0.4 Mya. Because both studies used target-capture with the same probe kit, the discrepancy could be caused by different bioinformatic pipelines (PHYLUCE; Faircloth, 2015 in Siniscalchi et al., 2023 vs HybPiper in this study) and/or different calibration points to build the time-calibrated tree. PHYLUCE is a conservative pipeline and is less efficient in recovering loci than HybPiper, which directly affects the estimation of branch lengths (Herrando-Moraira et al., 2018).

Our analysis suggests that the ancestral area of the American clade is either Southern North America (J) or Central North America (M; Fig. 3). In contrast, Siniscalchi et al. (2023) estimated Western North America as the ancestral area; such difference is probably due to the fact that in our tree the earliest diverging American clades correspond to Mexican and Central North American species that were not sampled in their work. Our BSM results show frequent exchanges between Western, Central and South North America, with Eastern North America being mainly a sink area, receiving at least two dispersals; however, such results should be taken with caution, given that several branches of this clade are very short and unsupported, as often happens in rapid radiations. Globally, our results support Siniscalchi et al. (2023) hypothesis that the North American radiation is the result of geographic speciation processes fostered by range expansion–contraction events during the Pleistocene cycles, as well as by habitat specialization leading to ecological speciation. Pollinator shifts may have also played a role in speciation processes of this clade: hummingbird pollination evolved multiple times in American *Cirsium* (Siniscalchi et al. 2023), and indeed most of the North American hummingbird lineages diversified also during the Pleistocene (Licón-Vera & Ornelas, 2017).

4.5. Taxonomic implications

The focus of this paper is not on the systematics of *Cirsium*, which we considered resolved in our previous work (Moreyra et al., 2023). However, in light of the comments by Del Guacchio et al. (2022) and Bureš et al., (2024) and the substantial additions to our sampling, we will outline some considerations that can be drawn from our results.

4.5.1. The problem of *Picnomon*

Our results (Figs. S1 and S2) support the monophyly of the genus *Cirsium*, except the coalescent analysis (Fig. S2), in which *Picnomon* is nested within *Cirsium*, being retrieved as sister to the subgenus *Lophiolepis*. *Picnomon acarna*, the only species of the genus, is morphologically similar to those of *Cirsium* and even it was first described as *Cirsium acarna* L. Incongruences found in our topologies for genus *Picnomon* could be the result of a hybrid origin, possibly between the ancestors of subgenera *Lophiolepis* and *Notobasis*. When a hybrid species shares the same ploidy level as the parental species (*Picnomon* $n = 16$; *Notobasis* $n = 17$; subg. *Lophiolepis* $n = 16$ – 17), hybridization events can be identified through methods based on phylogeny and sequence read-mapping (reviewed in Steenwyk et al., 2023). In phylogeny-based approaches, datasets comprising genetic loci from both the hybrid and parental species are anticipated to exhibit nearly equal support for two distinct topologies (reviewed in Steenwyk et al., 2023), and this is consistent with what we observe in our results: the concatenated-based tree (Fig. S1) shows *Picnomon* as sister to *Notobasis*, whereas the coalescence-based tree (Fig. S2) shows *Picnomon* as sister to *Cirsium* subg. *Lophiolepis*.

Therefore, we suggest again keeping *Picnomon* as a monotypic genus, probably hybridogenic.

As described in the introduction of this article, the circumscription of *Cirsium* is controversial and has been the object of intense debate in the last years (Ackerfield et al., 2020; Del Guacchio et al., 2022; Moreyra et al., 2023; Bureš et al., 2023; Bureš et al., 2024; Moreyra & Susanna, 2024). A major rearrangement was proposed by Del Guacchio et al. (2022), who splitted *Cirsium* into four genera. However, as we already pointed out in Moreyra et al. (2023) and Moreyra & Susanna, (2024), such a proposal relied on poorly resolved phylogenies with limited taxonomic sampling and mainly based on a few plastid regions already shown to be inadequate by Ackerfield et al. (2020). In contrast, our previous and current results rely on highly resolved phylogenies built on extensive datasets (986 nuclear and 183 plastid loci, summing up to 247, 251 and 117,823 nucleotides respectively) that support *Cirsium* as a monophyletic genus. The only problem with this classification is the position of two species, *C. italicum* and *C. vulgare*, both of them suspected to be hybridogenic (Del Guacchio et al., 2022; Moreyra et al., 2023; Bureš et al., 2023; Bureš et al., 2024).

4.5.2. Hybrids in *Cirsium*: *Cirsium italicum* and *C. vulgare*

In our previous study on the Carduus-*Cirsium* group (Moreyra et al., 2023) our results were robust, but our sampling did not include *Cirsium italicum*, which is now added to this new study. Del Guacchio et al. (2022) segregated *C. italicum* as a new genus, *Epytrachys*, and resuscitated Cassini's genus *Lophiolepis* for the rest of the species of subg. *Lophiolepis* (Table 1). They justified their proposal on the morphological singularity of *C. italicum* and the lack of monophyly of subg. *Lophiolepis* due to the position of *C. italicum* outside the main *Lophiolepis* clade. The incongruences recovered in our topologies confirm that *C. italicum* is indeed a very challenging species regarding its taxonomic placement: in the present study, *C. italicum* is sister to all other *Cirsium* species in the concatenated-based tree (Fig. S1) while in the coalescent tree (Fig. S2) it is placed within *Cirsium* subg. *Cirsium*, with high support in both trees. Such hard incongruence regarding the position of *C. italicum* points significantly to a hybrid origin, which could explain the morphological intermediacy of *C. italicum* between *Cirsium* and *Lophiolepis*.

As for *Cirsium vulgare*, it was reported to “jump” between subgenera, depending on the molecular dataset analyzed (nuclear vs. plastid) and the approach used (Ackerfield et al., 2020; Del Guacchio et al., 2022; Moreyra et al., 2023; Bureš et al., 2024). As a result, it was also suspected to be of hybrid origin (Ackerfield et al., 2020; Moreyra et al., 2023; Bureš et al., 2023) and finally proved to be one by Bureš et al., 2024. Our present results support this hypothesis (Figs. S1 and S2). In Moreyra et al. (2023), *C. vulgare* was placed in subg. *Lophiolepis* in the concatenated analyses while it was placed in subgenus *Cirsium* in the coalescent analyses. In our present study, using a larger dataset, it is placed in subgenus *Cirsium* in both trees. On morphological grounds, *C. vulgare* shows the distinctive foliar spines of subg. *Lophiolepis* and it is consistently classified in this subgenus. The conundrum has an easy explanation: this species is the result of a hybridization event between one species of subgenus *Cirsium* and one from subgenus *Lophiolepis* based on visual inspection of the phylogenetic position of paralogous copies in gene trees. As explained in the methods section, we examined each gene tree with paralogous copies to ensure that putative orthologous copies were correctly identified. In every gene tree that contained both orthologous and paralogous copies of *C. vulgare*, the putative orthologous copy was always placed within the clade corresponding to subg. *Cirsium*, whereas the paralogous copy was placed in subg. *Lophiolepis*. Our results and the fact of *C. vulgare* being tetraploid (Bureš et al., 2023 and references therein) support the hypothesis that this species is an allopolyploid (Bureš et al., 2024).

4.5.3. Hybrids and systematics

Hybrids between subgenera *Cirsium* and *Lophiolepis* are common: at least 12 known cases following Del Guacchio et al. (2022) who state:

“Numerous intergeneric hybrids have been described between *Lophiolepis* and *Cirsium* (especially *C. vulgare*)”. This figure of 12 is notably inferior to the frequent hybrids described within each subgenus, as it could be expected from the 7 Mya dating of the split of the subgenera (Fig. S3). Actually, according to Dirmenci (pers. comm.), hybrids between *Cirsium* and *Lophiolepis* are unknown in the eastern part of its area. Anyway, as already commented, hybridization between both subgenera is at the origin of *C. italicum* and *C. vulgare*; the fact that the two subgenera may create fertile hybrids is strong evidence of the closeness of the two groups, and supports the traditional circumscription of *Cirsium* first proposed by Miller (1768) and followed by most of authors until 2022.

Moreover, and regarding the taxonomic classification, the segregation of *C. italicum* as *Epytrachys* (Del Guacchio et al., 2022), and the recent proposal of segregating *C. vulgare* as another monotypic genus (Bureš et al., 2024), would leave subg. *Cirsium* as paraphyletic, since the Asiatic clade including *C. interpositum*, *C. lidjiangense*, *C. verutum* and *C. subulariforme* are placed as basal in the subgenus.

The case of the closely related subtribe Centaureinae is quite illustrative of our views on the classification of *Cirsium*. The large genus *Centaurea* is divided in three subgenera, namely *Centaurea*, *Cyanus* and *Lopholoma* (Hilpold et al., 2014), which constitute a well-supported clade in a recent phylogenomic analysis (Calleja et al., in prep.). Even if no hybrids have been hitherto found between subgenera of *Centaurea*, current classification (Susanna and García-Jacas, 2007; 2009; Hilpold et al., 2014) do not favor splitting the genus in three different genera. Thus, according to our own guidelines (supported by other Compositae specialists, e.g. Funk et al., 2009) when dealing with species-rich genera, we consider *Cirsium* a single genus with two subgenera, namely subg. *Cirsium* and subg. *Lophiolepis*.

CRedit authorship contribution statement

Lucía D. Moreyra: Writing – review & editing, Writing – original draft, Visualization, Validation, Software, Project administration, Methodology, Investigation, Formal analysis, Data curation, Conceptualization. **Alfonso Susanna:** Writing – review & editing, Validation, Supervision, Resources, Project administration, Investigation, Funding acquisition, Conceptualization. **Juan Antonio Calleja:** Writing – review & editing, Validation, Supervision, Investigation, Conceptualization. **Jennifer R. Ackerfield:** Writing – review & editing, Validation, Resources. **Turan Arabacı:** Resources. **Carme Blanco-Gavaldà:** Writing – review & editing, Software. **Christian Brochmann:** Writing – review & editing, Validation, Resources. **Tuncay Dirmenci:** Writing – review & editing, Resources, Investigation. **Kazumi Fujikawa:** Resources. **Mercè Galbany-Casals:** Writing – review & editing, Project administration, Funding acquisition. **Tiangang Gao:** Resources. **Abel Gizaw:** Resources. **Iraj Mehregan:** Resources. **Roser Vilatersana:** Writing – review & editing, Resources. **Juan Viruel:** Writing – review & editing, Software. **Bayram Yıldız:** Resources. **Frederik Leliaert:** Writing – review & editing, Resources. **Alexey P. Seregin:** Writing – review & editing, Resources. **Cristina Roquet:** Writing – review & editing, Visualization, Validation, Supervision, Software, Resources, Investigation, Conceptualization.

Funding

This work received financial support from the Spanish Ministry of Science, Innovation and Universities (PD2019-105583 GB-C21/AEI/h <https://doi.org/10.13039/501100011033>, Ph.D. grant PRE2020-093069), the Catalan government (“Ajuts a grups consolidats” 2021SGR00315), the National Natural Science Foundation of China (grant nos. 32270229), the Sino-Africa Joint Research Center (grant no. SAJC201614). The work of A.P.S. on the curation of dry plant material was supported by the Moscow State University assignment (project 121032500090-7).

Acknowledgements

Authors thank María Luisa Gutiérrez for providing technical support during the laboratory process and curators and technicians of the herbaria that provided material for the study as well as all collaborators that provided material from their own collections. Collection in Rwanda was done under Research permit No NCST/482/304/2022 and with the permission of Rwanda Development Board (RDB) Tourism and Conservation to collect in the Volcanoes National Park. We thank Prof. Elias Bizuru for allowing affiliation of M.G.-C. and J.A.C. to University of Rwanda, Dr. Richard Muvunyi from RDB for his support, the staff of the Volcanoes National Park for field assistance; and Beth Kaplin and the staff from the National Herbarium of Rwanda, as well as the staff of the Ellen DeGeneres Campus in Musanze, for logistic support.

Appendix A. Supplementary data

Supplementary data to this article can be found online at <https://doi.org/10.1016/j.jympev.2025.108285>.

Data Availability Statement

Raw sequences generated during this study were deposited in the NCBI Short Read Archive database (SRA) under the BioProject accession number PRJNA957074 (<https://www.ncbi.nlm.nih.gov/bioproject/?term=PRJNA957074>).

BioSample accession numbers for each sample can be found in the [Supplementary Materials](#) along with herbaria codes and voucher information (Table S1).

References

- Ackerfield, J., Susanna, A., Funk, V., Kelch, D., Park, D.S., Thornhill, A.H., Yildiz, B., Arabaci, T., Dirmenci, T., 2020. A prickly puzzle: Generic delimitations in the *Carduus*-*Cirsium* group (Compositae: Cardueae: Carduinae). *Taxon* 69, 715–738.
- Barres, L., Sanmartín, I., Anderson, C.L., Susanna, A., Buerki, S., Galbany-Casals, M., Vilatersana, R., 2013. Reconstructing the evolution and biogeographic history of tribe Cardueae (Compositae). *Amer. J. Bot.* 100, 867–882.
- Bolger, A.M., Lohse, M., Usadel, B., 2014. Trimmomatic: a flexible trimmer for Illumina Sequence Data. *Bioinform.* 30, 2114–2120.
- Bureš, P., Özcan, M., Šmerda, J., Micháliková, E., Horová, L., Pláčková, K., Šmarda, P., Elliott, T.L., Veselý, P., Čato, S., et al., 2023. Evolution of genome size and GC content in the tribe Carduinae (Asteraceae): Rare descending dysploidy and polyploidy, limited environmental control and strong phylogenetic signal. *Preslia* 95, 185–213.
- Bureš, P., Del Guacchio, E., Šmerda, J., Özcan, M., Bliznáková, P., Vavrinec, M., Micháliková, E., Veselý, P., Veselá, K., Zedek, F., 2024. Intergeneric hybrid origin of the invasive tetraploid *Cirsium vulgare*. *Plant Biol.* 26, 749–763.
- Burnham, K.P., Anderson, D.R., 1998. Model selection and multimodel inference: a practical information-theoretic approach. Springer, New York.
- Capella-Gutiérrez, S., Silla-Martínez, J.M., Gabaldón, T., 2009. trimAl: a tool for automated alignment trimming in large-scale phylogenetic analyses. *Bioinformatics* 25, 1972–1973.
- Charadze, A.L., 1963. *Cirsium* Mill. In: Bobrov EG, Cherepanov SK, (Eds.), E.G., Cherepanov, S.K., editors. *Flora of the USSR* (Vol. XXVIII, pp. 63–270). Moscow: Izdatel'stvo Akademii Nauk SSSR.
- Cornacchia, I., Agostini, S., Brandano, M., 2018. Miocene oceanographic evolution based on the Sr and Nd isotope record of the central mediterranean. *Paleoceanogr. Paleoclimatol.* 33, 31–47.
- Darriba, D., Posada, D., Kozlov, A.M., Stamatakis, A., Morel, B., Flouri, T., 2019. ModelTest-NG: a new and scalable tool for the selection of DNA and protein evolutionary models. *Mol. Biol. Evol.* 37, 291–294.
- Davis, P.H., Parris, S.B., 1975. *Cirsium* Mill. In: Davis, P.H. (Ed.), *Flora of Turkey and the East Aegean Islands*. Edinburgh University Press, Edinburgh, pp. 370–412.
- Davison, A., Chiba, S., Barton, N.H., Clarke, B., 2005. Speciation and gene flow between snails of opposite chirality. *PLoS Biol.* 3, e282.
- Candolle, A.P. de, Duby, J.E., 1828. *Botanicon gallicum* (2nd ed., Vol. 2). Paris: Veuve Bouchard-Huzard.
- Candolle, A.P. de, 1837. *Prodromus systematis naturalis regni vegetabilis*, vol. 6. Paris: Treuttel et Würtz.
- Del Guacchio, E., Bureš, P., Iamónico, D., Carucci, F., De Luca, D., Zedek, F., Caputo, P., 2022. Towards a monophyletic classification of Cardueae: restoration of the genus *Lophiolepis* (= *Cirsium* pp) and new circumscription of *Epirachys*. *Plant Biosyst.* 56, 1269–1290.
- Dupin, J., Matzke, N.J., Särkinen, T., Knapp, S.J., Olmstead, R.G., Bohs, L., Smith, S.D., 2017. Bayesian estimation of the global biogeographic history of the Solanaceae. *J. Biogeogr.* 44, 887–899.
- Eronen, J.T., Atabadi, M.M., Micheels, A., Karme, A., Bernor, R.L., Fortelius, M., 2009. Distribution history and climatic controls of the Late Miocene Pirkermian chronofauna. *Proc. Natl. Acad. Sci. USA* 106, 11867–11871.
- Etienne, R.S., Haegeman, B., Stadler, T., Aze, T., Pearson, P.N., Purvis, A., Phillimore, A. B., 2012. Diversity-dependence brings molecular phylogenies closer to agreement with the fossil record. *Proc. R. Soc. B Biol. Sci.* 279, 1300–1309.
- Faircloth, B.C., 2015. PHYLUCE is a software package for the analysis of conserved genomic loci. *Bioinformatics* 32, 786–788.
- Fér, T., Schmickl, R.E., 2018. HybPhyloMaker: target enrichment data analysis from raw reads to species trees. *Evol. Bioinform.* 14, 1–9.
- Fernández-Palacios, J.M., de Nascimento, L., Otto, R., Delgado, J.D., García-del-Rey, E., Arévalo, J.R., Whittaker, R.J., 2011. A reconstruction of Palaeo-Macaronesia, with particular reference to the long-term biogeography of the Atlantic island laurel forests. *J. Biogeogr.* 38, 226–246.
- Funk, V.A., Susanna, A., Stuessy, T.F., Bayer, R.J. (Eds.), 2009. *Systematics, Evolution, and Biogeography of Compositae*. IAPT, Vienna, Austria, pp. 293–313.
- Gehrke, B., Linder, H.P., 2014. Species richness, endemism and species composition in the tropical Afroalpine flora. *Alpine Botany* 124, 165–177.
- Gorospe, J.M., Monjas, D., Fernández-Mazuecos, M., 2020. Out of the Mediterranean region: worldwide biogeography of snapdragons and relatives (tribe Antirrhineae, Plantaginaceae). *J. Biogeogr.* 47 (11), 2442–2456.
- Herbert, T.D., Lawrence, K.T., Tzanova, A., Peterson, L.C., Caballero-Gill, R., Kelly, C.S., 2016. Late Miocene global cooling and the rise of modern ecosystems. *Nat. Geosci.* 9 (11), 843–847.
- Herrando-Moraira, S., Calleja, J.A., Carnicero-Campmany, P., Fujikawa, K., Galbany-Casals, M., García-Jacas, N., Im, H.-T., Kim, S.-C., Liu, J.-Q., López-Alvarado, J., López-Pujol, J., Mandel, J.R., Massó, S., Mehregan, I., Montes-Moreno, N., Pyak, E., Roquet, C., Sáez, L., Sennikov, A.N., Susanna, A., Vilatersana, R., 2018. Exploring data processing strategies in NGS target enrichment to disentangle radiations in the tribe Cardueae (Compositae). *Mol. Phylogenet. Evol.* 128, 69–87.
- Herrando-Moraira, S., Calleja, J.A., Galbany-Casals, M., García-Jacas, N., Liu, J.-Q., López-Alvarado, J., López-Pujol, J., Mandel, J.R., Massó, S., Montes-Moreno, N., Roquet, C., Sáez, L., Sennikov, A.N., Susanna, A., Vilatersana, R., 2019. Nuclear and plastid DNA phylogeny of tribe Cardueae (Compositae) with Hyb-Seq data: a new subtribal classification and a temporal diversification framework. *Mol. Phylogenet. Evol.* 137, 313–332.
- Herrando-Moraira, S., Roquet, C., Calleja, J.A., Chen, Y.S., Fujikawa, K., Galbany-Casals, M., García-Jacas, N., Liu, J.-Q., López-Alvarado, J., López-Pujol, J., Mandel, J.R., Mehregan, I., Sáez, L., Sennikov, A.N., Susanna, A., Vilatersana, R., Xu, L.S., 2023. Impact of the climatic changes in the Pliocene-Pleistocene transition on Irano-Turanian species. The radiation of genus *Jurinea* (Compositae). *Molec. Phylogenet. Evol.* 189, 107928.
- Hilpold, A., García-Jacas, N., Vilatersana, R., Susanna, A., 2014. Notas taxonómicas y nomenclaturales en Centaurea: propuesta de clasificación, descripción de secciones y subsecciones nuevas, y lista de especies de una sección Centaurea redefinida. *Collect. Bot.* 33, e001.
- Iwatsuki, K., 1995. Subtribe III Carduinae. In: Iwatsuki, K., Yamazaki, T., Boufford, D.E., Ohba, H. (Eds.), *Flora of Japan*. Kodansha, Tokyo.
- Johnson, M.G., Gardner, E.M., Liu, Y., Medina, R., Goffinet, B., Shaw, A.J., Zerega, N.J. C., Wickett, N.J., 2016. HybPiper: Extracting coding sequence and introns for phylogenetics from high-throughput sequencing reads using target enrichment. *Appl. Plant Sci.* 4, 1600016.
- Kadota, Y., 2012. Taxonomic Studies of *Cirsium* (Asteraceae) in Japan XXIII. A New Species from Hachioji, Tokyo Prefecture, Central Japan. *Bull. Nat. Mus. Nat. Sci. Ser. B, Bot.* 38, 1–10.
- Katoh, K., Toh, H., 2008. Recent developments in the MAFFT multiple sequence alignment program. *Brief. Bioinform.* 9, 286–298.
- Kelch, D.G., Baldwin, B.G., 2003. Phylogeny and ecological radiation of New World thistles (*Cirsium*, Cardueae - Compositae) based on ITS and ETS rDNA sequence data. *Mol. Ecol.* 12, 141–151.
- Kovar-Eder, J., Kvacek, Z., Martinetto, E., Roiron, P., 2006. Late Miocene to Early Pliocene vegetation of southern Europe (7–4Ma) as reflected in the megafossil plant record. *Palaeogeogr. Palaeoclimatol. Palaeoecol.* 238, 321–339.
- Kozlov, A., Darriba, D., Flouri, T., Morel, B., Stamatakis, A., 2019. RAXML-NG: a fast, scalable, and user-friendly tool for maximum likelihood phylogenetic inference. *Bioinformatics* 35, 4453–4455.
- Kück, P., Longo, G.C., 2014. FASconCAT-G: extensive functions for multiple sequence alignment preparations concerning phylogenetic studies. *Front. Zool.* 11, 81.
- Kumar, S., Stecher, G., Li, M., Knyaz, C., Tamura, K., 2018. MEGA X: molecular evolutionary genetics analysis across computing platforms. *Mol. Biol. Evol.* 35, 1547–1549.
- Landis, M.J., Matzke, N.J., Moore, B.R., Huelsenbeck, J.P., 2013. Bayesian analysis of biogeography when the number of areas is large. *Syst. Biol.* 62, 789–804.
- Li, H., Durbin, R., 2009. Fast and accurate short read alignment with Burrows-Wheeler Transform. *Bioinformatics* 25, 1754–1760.
- Licona-Vera, Y., Ornelas, J.F., 2017. The conquering of North America: dated phylogenetic and biogeographic inference of migratory behavior in bee hummingbirds. *BMC Evol. Biol.* 17, 126.
- Louca, S., Pennell, M.W., 2020. Extant time trees are consistent with a myriad of diversification histories. *Nature* 580 (7804), 502–505.
- Mai, D.H., 1995. *Tertiäre Vegetationsgeschichte Europas: Methoden und Ergebnisse*. Gustav Fischer Verlag, Jena.

- Mairal, M., Pokorný, L., Aldasoro, J.J., Alarcón, M., Sanmartín, I., 2015. Ancient vicariance and climate-driven extinction continental-wide disjunctions in Africa: the case of the Rand Flora genus *Canarina* (Campanulaceae). *Mol. Ecol.* 24, 1335–1354.
- Mandel, J.R., Dikow, R.B., Funk, V.A., Masalia, R.R., Staton, S.E., Kozik, A., Michels, R.W., Rieseberg, L.H., Burke, J.M., 2014. A target enrichment method for gathering phylogenetic information from hundreds of loci: an example from the Compositae. *Appl. Plant Sci.* 2, 1300085.
- Mandel, J.R., Dikow, R.B., Siniscalchi, C.M., Thapa, R., Watson, L.E., Funk, V.A., 2019. A fully resolved backbone phylogeny reveals numerous dispersals and explosive diversifications throughout the history of Asteraceae. *Proc. Natl. Acad. Sci. USA* 116, 14083–14088.
- Matzke, N.J., 2014. Model selection in historical biogeography reveals that founder-event speciation is a crucial process in island clades. *Syst. Biol.* 63, 951–970.
- Matzke, N.J., 2013 BioGeoBEARS: Biogeography with Bayesian (and Likelihood) Evolutionary Analysis in R Scripts. R Package. Available online: <https://github.com/nmatzke/BioGeoBEARS> (accessed in March 2022).
- T.G. McLay J.L. Birch B.F. Gunn W. Ning J.A. Tate L. Nauheimer E.M. Joyce L. Simpson Schmidt-Leubnig, A.N., Baker, W.J. and Forest, F. New targets acquired: Improving locus recovery from the Angiosperms353 probe set *Appl. Plant Sci.* 9 2021 e11420.
- Miller, P. 1768. The gardener's dictionary, (4th ed., Vol. 3). London: Printed for the author.
- Moore-Pollard, E.R., Jones, D.S., Mandel, J.R., 2024. Compositae-ParaLoss-1272: a complementary sunflower-specific probe set reduces paralogs in phylogenomic analyses of complex systems. *Appl. Plant Sci.* 12, e11568.
- Moreyra, L.D., Garcia-Jacas, N., Roquet, C., Ackerfield, J.R., Arabaci, T., Blanco-Gavaldà, C., Brochmann, C., Calleja, J.A., Dirmenci, T., Fujikawa, K., Galbany-Casals, M., Gao, T., Gizaw, A., López-Alvarado, J., Mehregan, I., Vilatersana, R., Yildiz, B., Leliart, F., Seregin, A.P., Susanna, A., 2023. African mountain thistles: three new genera in the *Carduus-Cirsium* group. *Plants* 12, 3083.
- Moreyra, L.D.; Susanna, A. Reply to Del Guacchio et al. The Genus *Lophiolepis* Is at Least as Well Supported as *Afrocarduus*, *Afrocardium*, and *Nuriaea*. Comment on “Moreyra et al. African Mountain Thistles: Three New Genera in the *Carduus-Cirsium* Group. *Plants* 2023, 12, 3083”. *Plants* 2024, 13, 3400.
- Morlon, H., Lewitus, E., Condamine, F.L., Manceau, M., Clavel, J., Drury, J., 2016. RPANDA: an R package for macroevolutionary analyses on phylogenetic trees. *Meth. Ecol. Evol.* 7, 589–597.
- Morlon, H., Robin, S., Hartig, F., 2022. Studying speciation and extinction dynamics from phylogenies: addressing identifiability issues. *Trends Ecol. Evol.* 37, 497–506.
- Nazaire, M., Wang, X.-Q., Hufford, L., 2014. Geographic origins and patterns of radiation of *Mertensia* (Boraginaceae). *Am. J. Bot.* 101, 104–118.
- Nee, S., Mooers, A.O., Harvey, P.H., 1992. Tempo and mode of evolution revealed from molecular phylogenies. *Proc. Natl. Acad. Sci. USA* 89, 8322–8326.
- Paradis, E., Schliep, K., 2019. ape 5.0: An environment for modern phylogenetics and evolutionary analyses in R. *Bioinformatics* 35, 526–528.
- Petrak F. 1979. *Cirsium* Mill. In: Rechinger KH, editor, *Flora Iranica*, vol. 139a. Graz: Akademische Druck- und Verlagsanstalt; p. 231–280.
- Pignatti, S., 1978. Evolutionary trends in Mediterranean flora and vegetation. *Vegetatio* 37, 175–185.
- Pillans, B., Chappell, J., Naish, T.R., 1998. A review of the Milankovitch climatic beat: template for Plio-Pleistocene sea-level changes and sequence stratigraphy. *Sed. Geol.* 122, 5–21.
- Ramallo, R.S., Brum da Silveira, A., Fonseca, P.E., Madeira, J., Cosca, M., Cachao, M., Fonseca, M.M., Prada, S.N., 2015. The emergence of volcanic oceanic islands on a low-moving plate: the example of Madeira Island, NE Atlantic. *Geochem. Geophys. Geosystems* 16, 522–537.
- Ree, R.H., Moore, B.R., Webb, C.O., Donoghue, M.J., 2005. A likelihood framework for inferring the evolution of geographic range on phylogenetic trees. *Evolution* 59, 2299–2311.
- Ree, R.H., Smith, S.A., 2008. Maximum likelihood inference of geographic range evolution by dispersal, local extinction and cladogenesis. *Syst. Biol.* 57, 4–14.
- Ronquist, F., 1997. Dispersal–vicariance analysis: a new approach to the quantification of historical biogeography. *Syst. Biol.* 46, 195–203.
- Shi, Z., Raab-Straube, E. von, Greuter, W., Martins, L., 2011. *Cardueae*. In: Wu, Z.Y., Raven, P.H., Hong, D.Y. (Eds.), *Flora of China* (Vols. 20–21, Pp. 42–194). Beijing: Science Press; St. Louis: Missouri Botanical Garden Press.
- Siniscalchi, C.M., Hidalgo, O., Palazzesi, L., Pellicer, J., Pokorný, L., Maurin, O., Leitch, I. J., Forest, F., Baker, W.J., Manderl, J.R., 2021. Lineage-specific vs. universal: a comparison of the Compositae1061 and Angiosperms353 enrichment panels in the sunflower family. *Appl. Plant Sci.* 9, e11422.
- Sepulchre, P., Ramstein, G., Fluteau, F., Schuster, M., Tercelin, J.J., Brunet, M., 2006. Tectonic uplift and Eastern Africa aridification. *Science* 313, 1419–1423.
- Siniscalchi, C.M., Ackerfield, J.R., Folk, R.A., 2023. Diversification and biogeography of North American thistles (*Cirsium*: *Carduoideae*: *Compositae*): drivers of a rapid continent-wide radiation. *Int. J. Pl. Sci.* 184, 322–341.
- Soto Gomez, M., Pokorný, L., Kantar, M.B., Forest, F., Leitch, I.J., Gravendeel, B., Wilkin, P., Graham, S.W., Viruel, J., 2019. A customized nuclear target enrichment approach for developing a phylogenomic baseline for *Dioscorea* yams (*Dioscoreaceae*). *Appl. Plant Sci.* 7, e11254.
- Stamatakis, A., 2014. RAxML version 8: A tool for phylogenetic analysis and post-analysis of large phylogenies. *Bioinform.* 30, 1312–1313.
- Steenwyk, J.L., Li, Y., Zhou, X., Shen, X.X., Rokas, A., 2023. Incongruence in the phylogenomics era. *Nat. Rev. Gen.* 24, 834–850.
- Susanna, A., Galbany-Casals, M., Romaschenko, K., Barres, L., Martin, J., Garcia-Jacas, N., 2011. Lessons from *Plectrocephalus* (*Compositae*, *Cardueae*-*Centaureinae*): ITS disorientation in annuals and Beringian dispersal as revealed by molecular analyses. *Ann. Bot.* 108, 263–277.
- Susanna, A., Garcia-Jacas, N., 2007. *Tribe Cardueae*. In: *The Families and Genera of Vascular Plants*, 8. Springer, Berlin/Heidelberg, Germany, pp. 123–146.
- Susanna, A.; Garcia-Jacas, N. *Cardueae* (*Carduoideae*). In: *Systematics, Evolution, and Biogeography of Compositae*; Funk, V.A., Susanna, A., Stuessy, T.F., Bayer, R.J., Eds.; IAPT: Vienna, Austria, 2009; pp. 293–313.
- Talavera, S., 2015. *Cirsium* Mill. In: Aedo, C., Herrero, A. (Eds.), *Flora iberica. Plantas vasculares de la Península Ibérica e Islas Baleares* (vol. 16, pp. 136–176). Madrid: Real Jardín Botánico Madrid (CSIC).
- Tamura, K., Battistuzzi, F.U., Billings-Ross, P., Murillo, O., Filipinski, A., Kumar, S., 2012. Estimating divergence times in large molecular phylogenies. *Proc. Natl. Acad. Sci. USA* 109, 19333–19338.
- Tamura, K., Qiqing, T., Kumar, S., 2018. Theoretical foundation of the RelTime method for estimating divergence times from variable evolutionary rates. *Mol. Biol. Evol.* 35, 1770–1782.
- Tao, Q., Tamura, K., Mello, B., Kumar, S., 2020. Reliable confidence intervals for RelTime estimates of evolutionary divergence times. *Mol. Biol. Evol.* 37, 280–290.
- Valente, L.M., Savolainen, V., Vargas, P., 2010. Unparalleled rates of species diversification in Europe. *Proc. R. Soc. B Biol. Sci.* 277 (1687), 1489–1496.
- Vitales, D., Garnatje, T., Pellicer, J., Valles, J., Santos-Guerra, A., Sanmartín, I., 2014. The explosive radiation of *Cheirolophus* (*Asteraceae*, *Cardueae*) in Macaronesia. *BMC Evol. Biol.* 14, 118.
- Watson, L.E., Siniscalchi, C.M., Mandel, J., 2020. Phylogenomics of the hyperdiverse daisy tribes: anthemideae, Astereae, Calenduleae, Gnaphalieae, and Senecioneae. *J. Syst. Evol.* 58, 841–852.
- Weitemier, K., Straub, S.C., Cronn, R.C., Fishbein, M., Schmickl, R., McDonnell, A., Liston, A., 2014. Hyb-Seq: Combining target enrichment and genome skimming for plant phylogenomics. *Appl. Plant Sci.* 2, 1400042.
- Wen, J., Nie, Z.-L., Ickert-Bond, S., 2016. Intercontinental disjunctions between eastern Asia and western North America in vascular plants highlight the biogeographic importance of the Bering land bridge from late Cretaceous to Neogene. *J. Syst. Evol.* 54, 469–490.
- Werner, K., 1976. *Cirsium* Mill. In: Tutin, T.G., Heywood, V.H., Burges, N.A., Valentine, D.H. (Eds.), *Flora Europaea*, Vol. 4. Cambridge University Press, Cambridge, pp. 232–242.
- Westerhold, T., Marwan, N., Drury, A.J., Liebrand, D., Agnini, C., Anagnostou, E., Barnett, J.S.K., Bohat, S.M., De Vrieschouwer, D., Florindo, F., Frederichs, R., Hodel, D.A., Holbourn, A.E., Kroon, D., Lauretano, V., Littler, K., Lourens, L.J., Lyle, M., Pálfi, H., Röhl, U., Tian, J., Wilkens, R.H., Wilson, P.A., Zachos, J.C., 2020. An astronomically dated record of Earth's climate and its predictability over the last 66 million years. *Science* 369, 1383–1387.
- Zachos, J., Dickens, G., Zeebe, R., 2008. An early Cenozoic perspective on greenhouse warming and carbon cycle dynamics. *Nature* 451, 279–283.
- Zhang, C., Rabiee, M., Sayyari, E., Mirarab, S., 2018. ASTRAL-III: polynomial time species tree reconstruction from partially resolved gene trees. *BMC Bioinform.* 19, 15–30.
- Zhao, L., Lu, H., Wang, H., Meadows, M., Ma, C., Tang, L., Lei, F., Zhang, H., 2020. Vegetation dynamics in response to evolution of the Asian Monsoon in a warm world: pollen evidence from the Weihe Basin, central China. *Glob. Planet. Change* 193, 103269.